ELSEVIER

Nuclear Instruments and Methods in Physics Research B 193 (2002) 798–803

NIM B
Beam Interactions with Materials & Atoms

www.elsevier.com/locate/nimb

Desorption of nanoclusters (2–40 nm) from nanodispersed metal and semiconductor layers by swift heavy ions

I. Baranov [a], P. Håkansson [b], S. Kirillov [a], J. Kopniczky [b], A. Novikov [a], V. Obnorskii [a], A. Pchelintsev [a], A.P. Quist [b], G. Torzo [c], S. Yarmiychuk [a,*], L. Zennaro [c]

[a] *V.G. Khlopin Radium Institute, 2-Murinskiy Ave. 28, 194021 St.Petersburg, Russia*
[b] *Uppsala University, P.O. Box 534, 5-757 21 Uppsala, Sweden*
[c] *University of Padova, via G. Colombo 3, 35127 Padova, Italy*

Abstract

New experimental data on the desorption of nanoclusters (2–40 nm) from nanodispersed layers of metals (Ag, Pt, In, Bi) and semiconductors (Ge, UO_2, PbS) by fission fragments (FF) are reported and compared to the previously obtained data on desorption of nanoclusters of gold. It is shown that the desorption of nanoclusters from nanodispersed layers of metals and semiconductors due to electronic processes induced by swift heavy ions is a universal phenomenon. The yield of the desorbed nanoclusters depends on the cluster material and cluster size as well as on the material of the target substrate and varies within the range from ~5 to ~0.001 FF^{-1}. The angular distributions of the nanoclusters do not depend on the cluster material, but only on the cluster size: the mean polar angle of desorption decreasing from 45° to 23° while cluster size increasing from 2 to 40 nm. The majority of the nanoclusters is desorbed in the form of molten, liquid droplets. The results are discussed.

PACS: 79.20.Rf; 61.82.Rx; 36.40.-c
Keywords: Nanodispersed metal targets; Fission fragment bombardment; Nanometer cluster desorption; Cluster angular distribution; Cluster yield

1. Introduction

It is well known that stopping of swift heavy ions in spatially constrained aggregates of metals results in strong degradation of nanodispersed layers [1]. This phenomenon was previously treated as "inelastic (electronic) sputtering" [2]. Then it was established that as a result of fission fragment (FF) bombardment of metal (Au) nanodispersed islet targets (islet size 2–22 nm) the islets are desorbed as intact particles – nanoclusters [3–6]. Lately physical and chemical properties of nanoparticles of various materials have been studied actively, since this is both of technological importance and fundamental interest [7]. Studies

* Corresponding author. Tel.: +7-812-545-43-70; fax: +7-812-247-80-95.
E-mail address: yarmiy@atom.nw.ru (S. Yarmiychuk).

0168-583X/02/$ - see front matter
PII: S0168-583X(02)00907-2

of the nanocluster desorption have also been extended to nanodispersed layers of a wide range of materials. In this work the FF induced desorption of nanoclusters (cluster size range 2–40 nm) of metals – Pt, Ag, In, Pd, semimetal Bi and semiconductors – Ge, PbS, UO_2 is studied for the first time. Change of the islet matter leads to change of some parameters which influence the desorption process, as for example, the primary energy losses in an islet or the thermal and electrical conductivity of an islet, that determine the life time of the islet excited state. The new results are compared to those previously obtained on the desorption of nanoclusters of gold within the same size range [5,6].

2. Experimental techniques

2.1. Targets

Islet layers of metals and semiconductors were prepared by vapor-deposition of the matter in vacuo onto thin substrates. Usually 1 μm Al films covered with ~5 μg/cm^2 carbon layer were used as substrates. Size distributions of islets were varied by varying deposition conditions, i.e. the mean thickness of the layer (1.5–10 μg/cm^2), the evaporation rate and the substrate temperature t_{depos}. The deposited islet layers were characterized by means of a transmission electron microscope (TEM) as described elsewhere [5,6]. Examples of the electron micrographs of islet layers of some substances are presented in Fig. 1. In order to estimate the influence of the substrate material on the desorption process several targets of Bi were prepared on different substrates (Al+C, Ni, Ag, Au, Ag+NaCl, Al_2O_3) under the same deposition conditions.

2.2. Irradiation of targets and analysis of the desorbed clusters

The targets were irradiated with FFs from a ^{252}Cf source in pass-through geometry in vacuo $\sim 5 \times 10^{-7}$ Torr. The energy range of FFs was 40–70 MeV, and the electronic stopping power range was 12–26 keV/nm depending on the target material [8]. Fluence of FFs varied from 2×10^{10} to 1×10^{12} cm^{-2} depending on the desorption

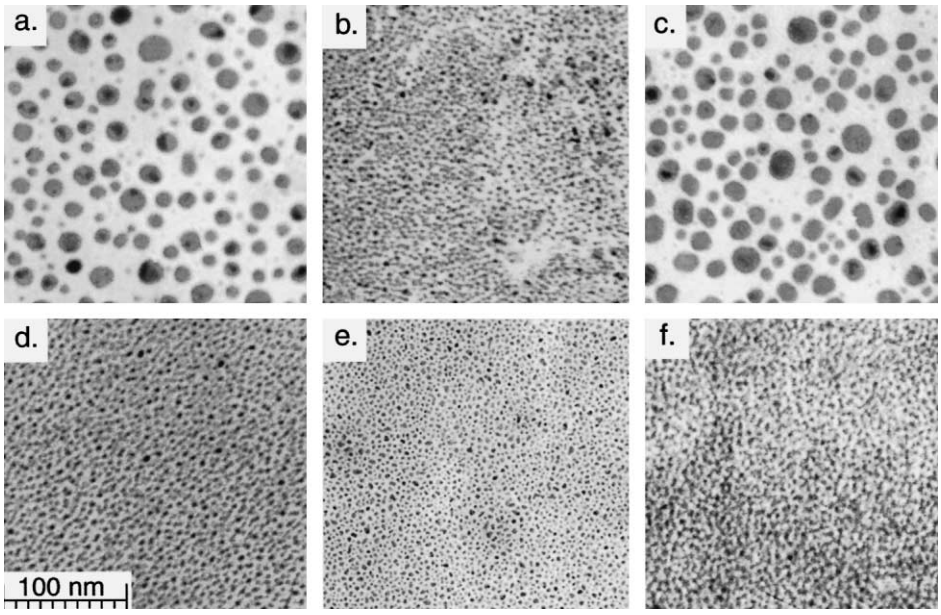

Fig. 1. TEM images of nanodispersed metal and semiconductor layers of (a) Ag, (b) Pt, (c) In, (d) Pd, (e) UO_2 and (f) Ge.

parameters to be determined. Registration and analysis of the desorbed nanoclusters involved the collector technique whose variants were described in detail in the works [5,6].

2.2.1. Sizes and masses of nanoclusters

To measure sizes and masses of the desorbed nanoclusters they were collected on two types of collectors – (1) carbon films on copper grids that were studied afterwards by TEM (Hitachi 600) and (2) freshly cleaved mica pieces that were studied by scanning force microscope (SFM, Nanoscope® III, Digital Instruments Inc. and Park Scientific Instruments). The areal density of clusters on the collectors was usually 10–50 nanoclusters/μm^2. TEM images were used to determine lateral size (D) distributions of the collected clusters, while SFM images were used to determine height (H) distributions thereof. The relationship of the mean height and of the mean lateral sizes of nanoclusters desorbed from a given target $\alpha = \langle H\rangle/\langle D\rangle$ was used to calculate the cluster mass distribution, quasi-spherical shape of the clusters being assumed [5].

2.2.2. Angular distributions and yields

According to the technique developed in [6] the desorbed clusters passed some drift (~10 mm) and were gathered onto a mosaic of TEM grids. TEM images made for these grids were used to determine the distribution of the areal density of the collected clusters over the collector. The latter was recalculated into the angular distribution of the desorbed clusters and the absolute desorption yield was evaluated, taking into account the experiment geometry and FF fluence. To measure the absolute yields of clusters of Pd, Bi, PbS, Ge having the order of magnitude of 10^{-1}–10^{-3} FF^{-1}, the clusters were collected onto one TEM grid placed at ~2 mm from the target and the areal density (n_x) of the clusters was determined. Then just the same was done for a reference nanodispersed target of gold with known yield ($Y_{ref.}$) of nanoclusters which had a similar size distribution. The absolute yield of cluster desorption from the target of interest (Y_x) was evaluated as $Y_x = Y_{ref.}(n_x/n_{ref.})$, where $n_{ref.}$ is the areal density of the gold clusters.

3. Results

3.1. Sizes and masses of desorbed nanoclusters

It was shown that desorption of nanoclusters occurs for all the islet layers of metals and semiconductors within the same size range as the islets on the targets (see Fig. 2). It is evident that Pt, Ag, Pd clusters, as well as previously observed gold clusters have regular round shape on the collector plane whereas most islets on the targets have slightly irregular shape (see Fig. 1). Size and mass ranges of the desorbed clusters of some materials are compiled in Table 1. Masses of Ge and UO_2 clusters were estimated basing on SFM measurements of the cluster heights because of insufficient contrast of TEM images and small cluster sizes, spherical cluster shape being assumed.

3.2. Angular distributions

Angular distributions of Pt, Ag, In nanoclusters within size range of 2.5–24 nm coincide within the experimental error with the angular distributions of gold clusters [6]. In general they are narrow, stretched normally to the target surface and are well-approximated by means of the same function $dn/d\Omega = g(\theta) \sim \exp(k \times \theta)\cos(\theta)$, $k = -2.2$ to -4.5 rad^{-1} for the cluster size 5–20 nm. The larger the cluster size is, the narrower the angular distribution is. Fig. 3 shows the results obtained for various 'target material–cluster size' combinations in coordinates: 'mean polar angle of cluster emission–mean size of the cluster desorbed'. One can see that regardless of the cluster matter all the experimental points are more or less uniformly distributed along a single curve.

3.3. Absolute yields

For nanodispersed targets of Pt, Ag and In the absolute yield of desorbed clusters was measured as a function of the mean cluster size (see Fig. 4). The same dependence for gold nanoclusters obtained previously [6] is also presented in Fig. 4. For targets of Pd, UO_2, PbS, Ge and Bi the values of the absolute yield of the desorbed nanoclusters are compiled in the Table 2. Influence of the substrate

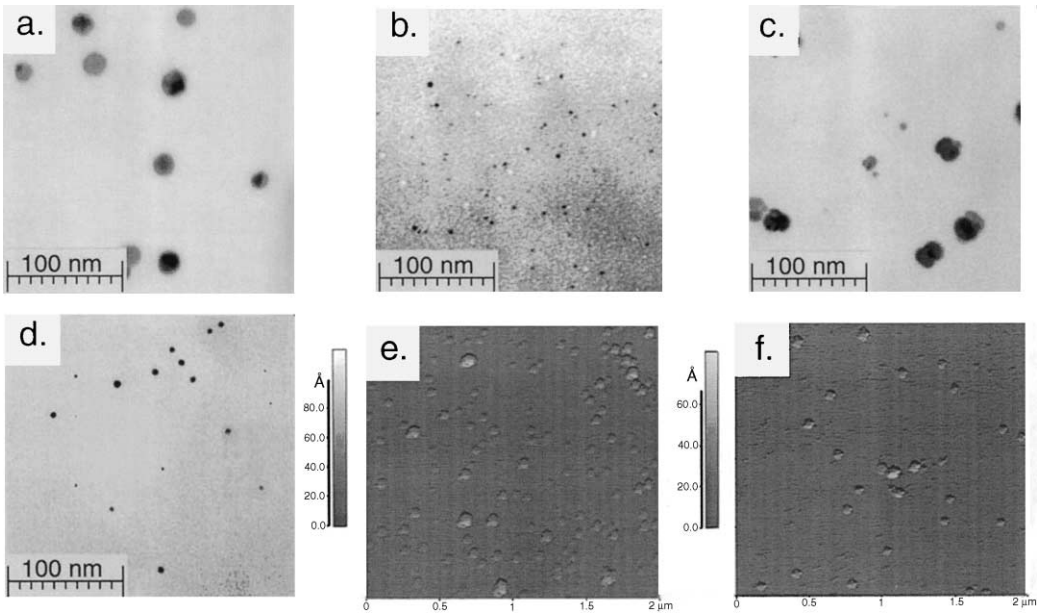

Fig. 2. TEM images of thin film carbon collectors with desorbed clusters of (a) Ag, (b) Pt, (c) In, (d) Pd and SFM image of mica collectors with desorbed clusters of (e) UO_2 and (f) Ge.

Table 1
Size and mass ranges of nanoclusters desorbed from various nanodispersed targets under FF bombardment

Cluster material	Cluster size range (nm)	$\langle H\rangle/\langle D\rangle$	Cluster mass range (amu)
Pt	1.0–5.5	0.93 (±10%)	1.0×10^4–1.4×10^6
Ag	3.0–24	0.80 (±10%)	1.7×10^5–4.8×10^7
In	4.0–29	0.67 (±10%)	1.0×10^6–4.0×10^7
Ge	3.0–5.0	–	5.0×10^4–2.0×10^5
UO_2	2.5–4.5	–	3.0×10^4–2.5×10^5

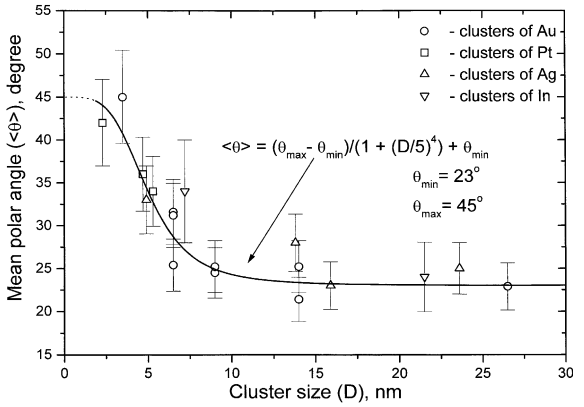

Fig. 3. Universal dependence of the mean polar angle of cluster desorption on the cluster size.

on the yield of the desorption was studied for the clusters of Bi. These results are also presented in Table 2.

4. Discussion

The main result of this work is that desorption of nanoclusters from the nanodispersed layers under FF bombardment is observed for a wide range of materials: metals (Pt, Ag, In, Pd), semimetal Bi and semiconductors (Ge, PbS, UO_2). This allows us to conclude that the desorption of nanoclusters from nanodispersed layers caused by a single swift heavy ion is a universal phenomenon.

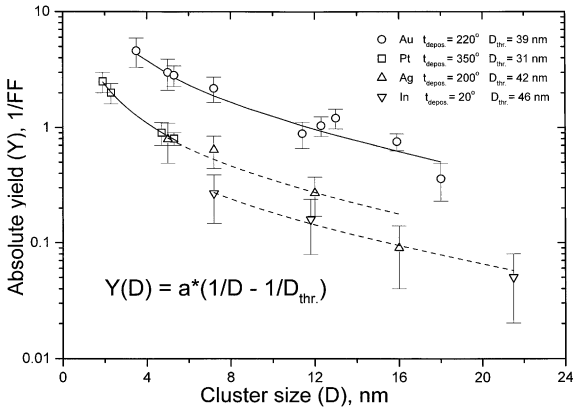

Fig. 4. Dependencies of the absolute cluster yield of Au, Pt, Ag and In on the cluster size (t_{depos} is the temperature of the target substrates during deposition of the islet layers, D_{thr} is the estimated desorption size threshold).

The following common features were observed for the process of desorption of nanoclusters of different materials:

(a) Sizes of the desorbed nanoclusters are approximately the same as those of the target islets. In general, size and mass ranges of the clusters desorbed were 2–40 nm and 10^4–10^8 amu respectively.

(b) In most cases the nanocluster desorption is accompanied by a change in the nanocluster shape: islets having irregular shape are transformed into nanoclusters with regular round shape, which is apparently connected with the islet heating and melting, i.e. these clusters are desorbed in the form of liquid nanodroplets. When the cluster size exceeds ~25 nm, non-round shaped clusters begin to appear, the relative number thereof depending on the melting point of the cluster material. It is probable that in these cases the energy deposited into the islets by FFs is sufficient to desorb the islets but not to melt them.

(c) The character of the detachment of the nanoclusters of different materials from the target substrate is the same. The angular distribution is defined solely by the size of the desorbed nanoclusters and does not depend on the cluster material (see Fig. 3). This result indicates the important role of the substrate, which provides the directional momentum perpendicular to the surface in the islet ejection process.

(d) The absolute yield of nanoclusters of different materials (Au, Ag, Pt, In) similarly decreases with the increase of the mean cluster size (see Fig. 4). Dependencies of the yield versus the mean nanocluster size in the general form are very well described by the function $Y(D) = A(1/D - 1/D_{thr})$, where D_{thr} is interpreted as the size threshold of the desorption. Possible origins of the desorption size threshold are considered in [6]. Fitting to the experimental points (see Fig. 4) allowed for estimating the D_{thr} values for the FF induced desorption of nanoclusters of Au, Ag, Pt, In as 39, 42, 31 and 46 nm, respectively. With respect to the desorption yield it is also important to note that we observed the yields >1 FF^{-1} for Pt and Ag

Table 2
Absolute yield Y of FF induced desorption of some nanocluster spices from nanodispersed layers of metals and semiconductors deposited on various substrates at the various substrate temperature t_{depos}

Cluster material	Substrate	t_{depos} (°C)	Cluster size range (nm)	Y (1/FF)
Au	Al + C	20	3–5	5.6 ± 1.1
Pd	Al + C	250	1.5–3	0.5 ± 0.3
UO_2	Al + C	300	1.5–4.5	0.4 ± 0.2
PbS	Al + C	250	1.5–5	0.25 ± 0.15
Ge	Al + C	180	3–5	0.10 ± 0.08
Bi	Al + C	200	5–10	~0.02*
Bi	Ag + NaCl	200	5–10	0.2 ± 0.1
Bi	Al_2O_3	200	5–10	0.10 ± 0.08
Bi	Ni	200	5–10	~0.02*
Bi	Ag	200	3–5	~0.005*
Bi	Au	200	1.5–3	~0.001*

* The accuracy of the yield measurements was of about factor of 2.

clusters sized at $D < 5$ nm, that is very similar to what had been observed for nanoclusters of gold in [6], i.e. islets can be desorbed without being passed through by a projectile.

In general the absolute yield of the nanocluster desorption varies within a very wide range – from $\sim$5 to $\sim$0.001 FF^{-1}. In addition to the cluster size it also depends on a number of factors, e.g.

(i) the nanocluster material that determines at least the value of the electronic energy losses of FFs in the irradiated islets (for the cluster materials involved they varied from 12 to 26 keV/nm) and adhesion of the islets to the target substrate;
(i) the material of the substrate that influences the islet-substrate adhesion too. It may also control the leakage of hot electrons from an excited islet to the substrate through the islet–substrate contact area. The data on the desorption of nanoclusters of Bi show the trend of increasing of the desorption yield with decreasing of electrical conductivity of the substrate material. This increase can reach up to two orders of magnitude with application of dielectric substrates (see Table 2).

The applied aspects of this work are connected with the development of the new desorption method of producing nanoclusters of different matters in the free state, including beams of accelerated nanocluster ions within the size range of 2–40 nm in the form of liquid nanodroplets. They may be used both for studying size effects in phase transitions in matter [9] and interaction of the accelerated clusters with the surface [10], as well as in fabrication of a new class of nanostructured solids and devices [11]. Use of different materials as substrates for nanodispersed layers will make it possible to vary the desorption yields and nanocluster beam intensities related thereto, within a wide range.

Acknowledgements

This work was supported by a grant from the International Science and Technology Center (ISTC project # 902-98).

References

[1] H. Andersen, H. Knudsen, H. Petersen, J. Appl. Phys. 49 (1978) 5638.
[2] I. Baranov, Yu Martynenko, S. Tsepelevich, Yu Yavlinskii, Sov. Phys. Usp. 31 (1988) 1015.
[3] I. Baranov, A. Novikov, V. Obnorskii, S. Tsepelevich, B. Kozlov, I. Pilyugin, Nucl. Instr. and Meth. B 65 (1992) 177.
[4] V.-T. Nguyen, K. Wien, I. Baranov, A. Novikov, V. Obnorskii, Rapid Commun. Mass-Spectrom. 10 (1996) 1463.
[5] I. Baranov, A. Novikov, V. Obnorskii, C. Reimann, Nucl. Instr. and Meth. B 146 (1998) 154.
[6] I. Baranov, S. Kirillov, A. Novikov, V. Obnorsky, A. Pchelintsev, S. Yarmijchuk, Nucl. Instr. and Meth. B 183 (2001) 232.
[7] J.H. Fendler (Ed.), Nanoparticles and Nanostructured Films: Preparation Characterzation and Applications, Wiley–VCH, Weinheim, 1998.
[8] J. Zigler, J. Biersack, The Stopping and Range of Ions in Solids, Pergamon Press, New York, 1990.
[9] D. Gerion, A. Hirt, I.M. Billas, A. Chatelain, W.A. de Heer, Phys. Rev. B 62 (2000) 7491.
[10] B. Pauwels, G. Van Tendeloo, W. Bouwen, L. Teil Kuhn, P. Lievens, H. Lei, M. How, Phys. Rev. B 62 (2000) 10383.
[11] P. Milani, P. Piseri, E. Barborini, A. Podesta, C. Lenardi, J. Vac. Sci. Technol. A 19 (2001) 2025.